




## Article

# Identification Algorithm and Improvement of Modal Damping Ratios for Armature Assembly in a Hydraulic Servo-Valve with Magnetic Fluid

Jinghui Peng <sup>1,2</sup>, Yayun Zhang <sup>1</sup>, Songjing Li <sup>1,\*</sup>, Wen Bao <sup>3</sup> and Yutaka Tanaka <sup>4</sup><sup>1</sup> Department of Fluid Control and Automation, Harbin Institute of Technology, Harbin 150001, China<sup>2</sup> State Key Laboratory of Fluid Power and Mechatronic Systems, Zhejiang University, Hangzhou 310027, China<sup>3</sup> School of Energy Science and Engineer, Harbin Institute of Technology, Harbin 150001, China<sup>4</sup> Faculty of Engineering and Design, Hosei University, Tokyo 102-8160, Japan

\* Correspondence: lisongjing@hit.edu.cn; Tel.: +86-451-8641-8318

**Abstract:** The high-frequency vibration and resonance of armature assembly in the hydraulic servo valve are the main reasons for instability and failure. Magnetic fluid (MF) operating in the squeeze mode can be taken as an effective damper for resonance suppression in the servo valve. Due to excitation difficulty and the low signal-to-noise ratio of high-frequency vibration signals, the capability of MF to modify multiple-order modal damping ratios in a multi-degree-of-freedom system is still unclear. To reveal the mechanism of magnetic fluid for improving modal damping ratios, an algorithm for modal damping ratio identification is proposed. The modal damping ratios of the armature assembly with and without magnetic fluid are identified based on the tested resonance free decay responses. Four resonance frequencies of armature assembly are observed, and the corresponding damping ratios are identified. The equivalent modal damping ratios due to squeeze flow of MF are obtained. The results show that the proposed algorithm can identify damping ratios with an accuracy of up to 98.79%. The damping ratios are improved by double or more due to the magnetic fluid, and the maximum resonance amplitudes are significantly reduced by 65.2% (from 916.5  $\mu\text{m}$  to 318.6  $\mu\text{m}$ ).



**Citation:** Peng, J.; Zhang, Y.; Li, S.; Bao, W.; Tanaka, Y. Identification Algorithm and Improvement of Modal Damping Ratios for Armature Assembly in a Hydraulic Servo-Valve with Magnetic Fluid. *Energies* **2023**, *16*, 3419. <https://doi.org/10.3390/en16083419>

Academic Editor: Tapas Mallick

Received: 18 November 2022

Revised: 22 March 2023

Accepted: 12 April 2023

Published: 13 April 2023



**Copyright:** © 2023 by the authors. Licensee MDPI, Basel, Switzerland. This article is an open access article distributed under the terms and conditions of the Creative Commons Attribution (CC BY) license (<https://creativecommons.org/licenses/by/4.0/>).

**Keywords:** squeeze flow; magnetic fluid; resonance suppression; modal damping ratio; hydraulic servo valve

## 1. Introduction

The electro-hydraulic servo technology is an important drive and transmission technology which is widely used in the national defense industries and modern production areas [1,2]. As the necessary key component of the electro-hydraulic servo system, the operational stability of the servo valve influences the reliable operation of the whole servo system significantly. The problem of instability and failure caused by self-excited noise in the servo valves is the most significant and potential hazard for electro-hydraulic servo systems, which require a high performance in the areas of defense, aerospace, aircraft, etc. [3–5]. Wang et al. [6] developed a dynamic model of a jet pipe servo valve to analyze the reliability and reliability sensitivities under a random vibration environment. The flow field and cavitation phenomena inside a deflector jet servo valve under different supply pressure conditions are investigated numerically and experimentally in [7]. The mechanism of squeal noise in a flapper-nozzle servo valve was explored from the hydraulic energy system perspective by Chen et al. [8]. It can be seen that conventional vibration suppression measures mainly focus on the structure optimization of armature assembly or flow field. However, with changes in the working conditions, the frequency of pressure pulsation in the flow field is prone to uncertainty, which means these methods are not universal. Thus, the squeal noise issue of the servo valve in the industry is still far from being resolved.

Here, magnetic fluid becomes one potential solution for the instability problem in servo valves. Magnetic fluid is a class of magneto-sensitive smart soft materials, which is generally prepared by dispersing nano-sized magnetizable particles into different magnetically insulated fluids, such as ester or water [9–11]. Due to excellent magneto-viscosity, inhibited sedimentation, and stability properties, MF has a wide range of applications in damping devices for structure vibration control [12–14]. Especially, with lower density and smaller size, the  $\text{Fe}_3\text{O}_4$ -based MF exhibits more stable characteristics while keeping sufficient magnetic saturation [15,16]. When MF works in squeeze mode, the large damping force can be generated even in small motion because of the squeeze strengthening effect [17–19]. Therefore, the squeeze flow of MF is attracting more and more attention from researchers [20,21]. Shafahi et al. [22] numerically investigated the squeeze flow dynamics and squeeze force evolution of a non-Newtonian fluid between two parallel disks. The squeeze strengthening effect of a magnetorheological fluid with  $\text{Fe}_3\text{O}_4$  addition was studied theoretically and experimentally by Wang et al. [23]. The results show that a high braking torque can be reached under the action of axial or radial squeezing. The mechanical characteristics of magnetorheological fluids in squeeze mode were investigated experimentally in [24]. It has been found that the magnetic field strengths, viscosity, and squeeze velocity are the dominant factors of the squeeze force.

When MF is applied in a two-stage servo valve, it is filled into the working gaps between the armature and cores in the torque motor (as shown in Figure 1). Large damping forces can be generated and applied on the armature due to the squeeze flow. The resonance amplitudes of the armature assembly can be reduced greatly, and the self-excited high-frequency noise in the servo valve can be noticeably suppressed. This has been proven in some of the previous studies [25–27]. The studies have shown that the function of MF in the working gaps of the torque motor can be simplified as a linear spring and viscosity damper. However, in a multi-degree-of-freedom (MDOF) system, the capability of MF to modify high-order modal damping ratios (under several thousand Hz) is still unclear. Thus, it is essential and valuable to find out the mechanism of MF for improving modal damping ratios and suppressing the specific resonance amplitude in an MDOF system.

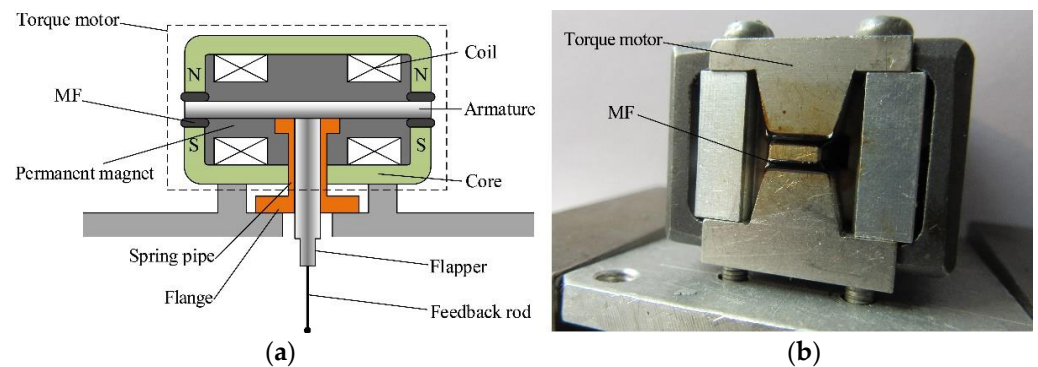


**Figure 1.** Construction and photograph of armature assembly in a hydraulic servo valve with MF. (a) Construction; (b) photograph.

Here, the estimation of modal damping ratios is also an essential part of the prediction of the structural dynamic response, the analysis of the energy dissipation source, and the evaluation of vibration suppression capability. Generally, the error in the identification of modal damping ratios is considerably larger compared to other modal parameters such as natural frequencies and vibration modes. It becomes more difficult for high-frequency vibration signals with lower signal-to-noise ratio. Thus, identification methods for modal damping ratios are gradually becoming a research focus, especially in engineering fields [28–30]. To reduce identification error, Tran et al. [31] identified damping ratios of bridge structures through different frequency-domain and time-domain methods. A collaborative solution employing multiple identification algorithms in a ranking-based manner

was innovatively proposed. A blind modal identification method based on enhanced sparse component analysis was developed to improve the accuracy of modal damping ratio identification in [32]. The effectiveness was demonstrated through the 10-DOF system using only two measurements. The performances of multiple correlation function-based methods were investigated by Sun et al. to present an effective tool for modal damping ratio estimation [33]. The results show that the time-frequency methods exhibit the best performance in damping estimation.

Being different from previous works, the aim of the paper is to propose an algorithm for the identification of high-order modal damping ratios, and to investigate the mechanism of magnetic fluid for improving modal damping ratios of the armature assembly. The study is based on the resonance free decay response and Fourier series fitting method. The modal damping ratios of the armature assembly with and without MF are obtained using a proposed identification algorithm after the dynamic test. Then, the effect of MF on modal damping ratios is analyzed to explain the damping capability of MF on the resonance suppression.

## 2. Working Principle of the Armature Assembly with MF

The construction and picture of the armature assembly with MF are shown in Figure 1. The armature assembly, which includes an armature, spring pipe, flapper, and feedback rod, is a crucial component of the servo valve to transfer a mechanical signal to a hydraulic signal. The vibration and deformation of the flapper and feedback rod may drastically affect the flow field and flow control characteristics of the main valve. More seriously, the fracture of the spring pipe caused by the resonance of the armature assembly may lead to the leakage of hydraulic oil and failure of the servo valve directly.

As the electro-mechanical mechanism of the servo valve, the torque motor moves the armature assembly to a rotation angle after a current is supplied to the motor. When the power of the torque motor is off, the armature will stay at the middle position due to the work of the permanent magnets. Because the permanent magnetic field always exists in the working gaps of the torque motor, no matter whether the torque motor is powered on or off, the squeeze film of MF is always kept in the working gaps and no sealing needs to be adopted. Therefore, it is very easy and convenient to apply MF in the gap between the torque motor armature and the cores.

The MF filled in the working gaps of the torque motor is exposed to a magnetic field generated by the electric magnets and the permanent magnets. The apparent viscosity of MF can be increased obviously in milliseconds because of the magnetization effect. The resulted damping forces due to the squeeze flow of MF are exerted on the end of the armature when the armature assembly rotates.

The existence of the squeeze film of MF provides a significant guarantee to maintain the stability of the servo valve by resisting the vibration of the armature assembly. Thus, stable control of the servo valve can be achieved.

## 3. Proposed Algorithm for Modal Damping Ratios Identification

### 3.1. Methodology

For a linear MDOF system, the resonance free decay response of the  $i$ th mode can be described as

$$x_i(t) = A_i e^{-\zeta_i \omega_i t} \cos(\omega_{di} t + \varphi_i), \quad (1)$$

where  $\omega_i$  and  $\omega_{di}$  are the undamped and damped natural frequencies of the  $i$ th mode, and  $A_i$ ,  $\zeta_i$  and  $\varphi_i$  are the amplitude, damping ratio, and phase of the  $i$ th mode, respectively.

To identify the  $i$ th damping ratio, a fitting function is given by

$$f_1(t) = a_1 + b_1 \cos(\omega_{di} t) + c_1 \sin(\omega_{di} t), \quad (2)$$

where  $a_1$ ,  $b_1$  and  $c_1$  are the coefficients of the function which can be identified by the Fourier series fitting method. Thus, the average amplitude of signal  $x_i(t)$  can be calculated as

$$\bar{A}_i = \sqrt{b_1^2 + c_1^2}, \quad (3)$$

Then, another fitting function is given by

$$f_2(t) = a_2 + b_2 e^{-\sigma_i t} \cos(\omega_{di} t) + c_2 e^{-\sigma_i t} \sin(\omega_{di} t), \quad (4)$$

where  $\sigma_i$  is the attenuation coefficient, and  $a_2$ ,  $b_2$ , and  $c_2$  are the coefficients of the function which can also be identified through the Fourier series fitting method when  $\sigma_i$  is specified. Thus, the amplitude of the  $i$ th mode can be calculated as

$$A_i = \sqrt{b_2^2 + c_2^2}, \quad (5)$$

For signal  $x_i(t)$ , there exists a mathematical relationship between  $\bar{A}_i$  and  $A_i$ :

$$\bar{A}_i = \frac{A_i(e^{-\sigma_i \Delta t} - 1)}{-\sigma_i \Delta t}, \quad (6)$$

where  $\Delta t$  is the time length of the signal  $x_i(t)$ .

Now, the target of the problem is to find the optimal solution of  $\sigma_i$  which has

$$E = \left| \sqrt{b_1^2 + c_1^2} - \frac{A_i(e^{-\sigma_i \Delta t} - 1)}{-\sigma_i \Delta t} \right| = \min, \quad (7)$$

Then, the  $i$ th damping ratio can be written as

$$\zeta_i = \frac{\sigma_i}{\omega_i}, \quad (8)$$

For a lightly damped system, we can assume  $\omega_i = \omega_{di}$ .

The equation of motion of the  $i$ th mode in modal coordinates can be described as

$$J_i(\ddot{q}_i + 2\zeta_i \omega_i \dot{q}_i + \omega_i^2 q_i) = \Phi_i^T T, \quad (9)$$

where  $T$  represents the generalized force matrix, and  $J_i$ ,  $q_i$ , and  $\Phi_i$  represent the modal inertia parameter, modal displacement, and modal shape of the  $i$ th mode, respectively.

Using the identified damping ratios,  $q_i$  in Equation (9) can be solved. Then, the structure dynamics can be obtained using the modal superposition method.

### 3.2. Model Verification

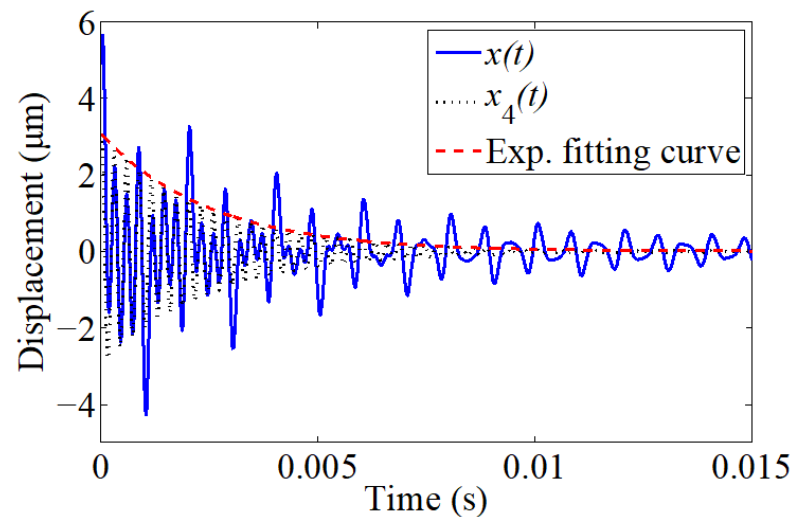
Due to the non-linearity of the servo valve torque motor, the real resonance free decay response may include multi-frequency components. Thus, the modal damping ratio estimation is more challenging, especially for higher order resonance frequencies. To validate the identification accuracy, a simulated resonance free decay response at 3500 Hz of a 4-degree-of-freedom system is given by

$$x(t) = \sum_{i=1}^4 x_i(t) = \sum_{i=1}^4 A_i e^{-2\pi f_i \zeta_i t} \cos(2\pi f_{di} t + \varphi_i) + B y(t), \quad (10)$$

The values of the simulation parameters in Equation (10) are listed in Table 1. Using the proposed identification method, the damping ratio of the resonance frequency component  $x_4(t)$  can be identified to be 0.0182, with an identification error of 1.11%. The identification results are shown in Figure 2.

**Table 1.** The values of the simulation parameters in Equation (10).

$i$	$A_i$ ( $\mu\text{m}$ )	$\zeta_i$ (%)	$f_i$ (Hz)	$\varphi_i$ (rad)
1	1	9.10	500	$\pi/2$
2	1	0.90	1500	$\pi/5$
3	1	0.90	2500	$\pi/4$
4	3	1.80	3500	$\pi/3$

**Figure 2.** Identified exponential decay curve vs. original signals.

The calculation results of the fourth-order modal damping ratio for different noise amplitudes  $B$  (1  $\mu\text{m}$ , 2  $\mu\text{m}$ , and 3  $\mu\text{m}$ ) are shown in Table 2. It can be seen from Table 2 that the identification error of the damping ratio increases with the increase in the noise amplitude, but, within a certain noise range, the identification results still have high accuracy.

**Table 2.** Identified damping ratios with different noise amplitudes.

$B$ ( $\mu\text{m}$ )	Theoretical Value (%)	Identified Value (%)	Error (%)	Accuracy (%)
1	0.19	0.1876	1.26	98.74
2	0.19	0.1851	2.58	97.42
3	0.19	0.1825	3.95	96.05

By setting the noise amplitude  $B$  as 3  $\mu\text{m}$ , the fourth-order steady-state amplitude  $A_4$  is varied as 0.5  $\mu\text{m}$ , 1  $\mu\text{m}$ , and 10  $\mu\text{m}$ , respectively. The calculation results of the fourth-order modal damping ratio are shown in Table 3. It can be seen from Table 3 that in the case of a low signal-to-noise ratio, the damping ratio identification error decreases with the increase in the steady-state amplitude of the target mode. Therefore, this method has high identification accuracy for the free decay response at the resonance frequency.

**Table 3.** Identified damping ratios with different steady-state amplitudes.

$A_4$ ( $\mu\text{m}$ )	Theoretical Value (%)	Identified Value (%)	Error (%)	Accuracy (%)
0.5	0.19	0.1469	22.68	77.32
1	0.19	0.168	11.58	88.42
10	0.19	0.1877	1.21	98.79

#### 4. Experimental Setup and Procedure

Considering the fragility of the spring pipe with a thickness of 60  $\mu\text{m}$ , the electromagnetic excitation approach and non-contact measurement technique are adopted to acquire the resonance free decay responses of the armature assembly. The experimental setup is shown in Figure 3. The torque motor is driven by a controllable servo amplifier (custom-built, Harbin Institute of Technology, Harbin, China). The communication between the computer and amplifier is realized through a digital–analog converter (PCI-1710, Advantech Co., Ltd., Kunshan, China). A laser displacement sensor (LK-G5000, Keyence Company, Osaka, Japan) is used to measure the dynamic responses of the feedback rod. The applied MF (custom-built, Heilongjiang Provincial Institute of Chemical Engineering, Harbin, China) in the experiment is a kind of ester-based  $\text{Fe}_3\text{O}_4$  magnetic fluid with a saturation magnetization of 0.045 T.

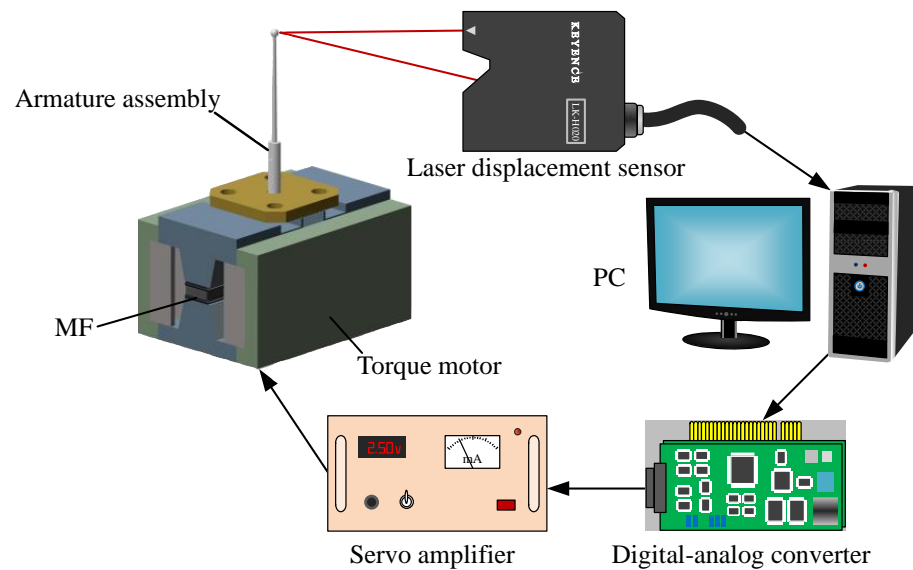


**Figure 3.** Experimental setup for driving torque motor and measuring dynamic response of armature assembly.

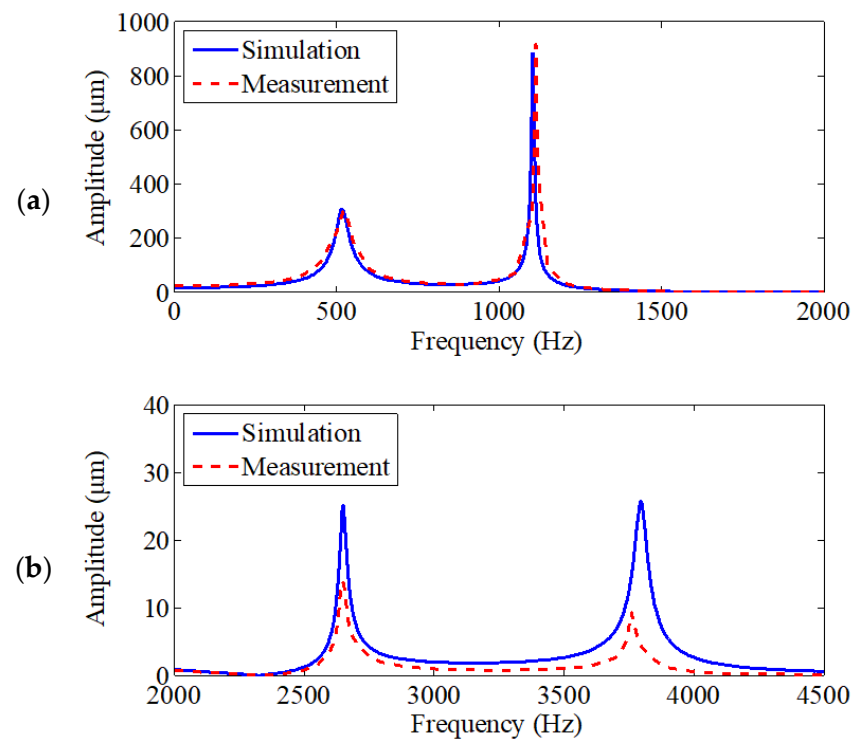
Firstly, the amplitude–frequency response of the torque motor is tested using the point-to-point sine sweep method to obtain the resonance frequencies of the armature assembly. The frequency of the input current signal varies from 0 to 4500 Hz, and the amplitude is kept to be constant. The sampling frequency of the displacement sensor is chosen to be as high as 100 kHz to acquire the high-frequency responses accurately.

Then, the resonance free decay response of each mode is acquired by driving the torque motor using a sinusoidal current signal at resonance frequency and turning off the power after a steady-state response is approached. The magnetic induction intensity in the working gaps is higher than 0.2 T when the control current varies sinusoidally. Thus, the particles in MF are always magnetized to saturation, even when the torque motor is powered off.

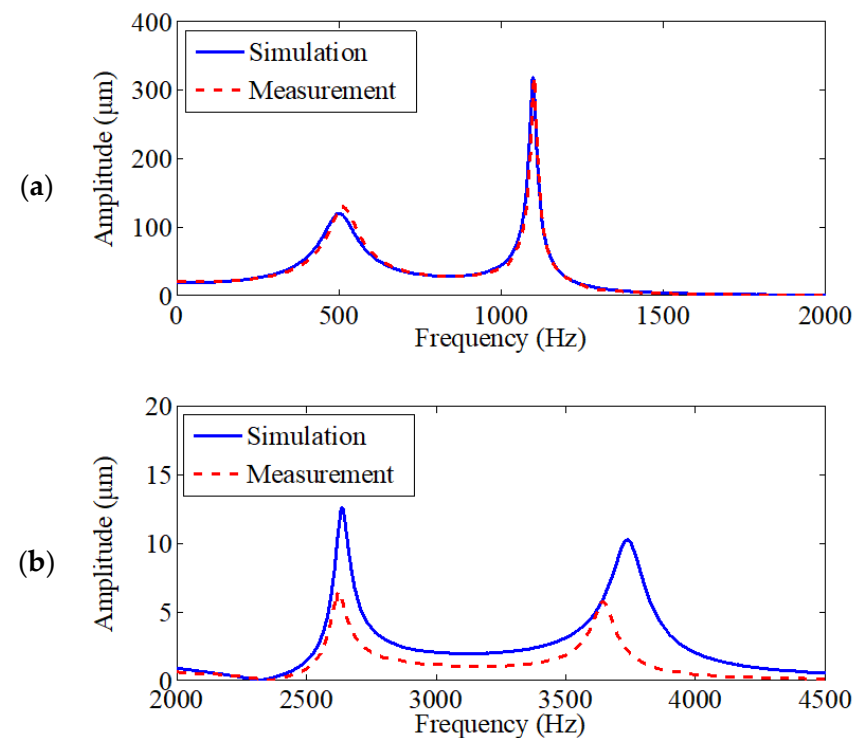
#### 5. Results and Discussion

##### 5.1. Improvement of Modal Damping Ratios

The tested amplitude–frequency response curves are shown in Figures 4 and 5. It can be seen that there are four vibration modes in the whole frequency range for both of the conditions before and after MF is applied. The identified resonance frequencies are listed in Table 4.



**Figure 4.** Calculated and tested amplitude–frequency response of torque motor without MF. (a) 0~2000 Hz; (b) 2000~4500 Hz.

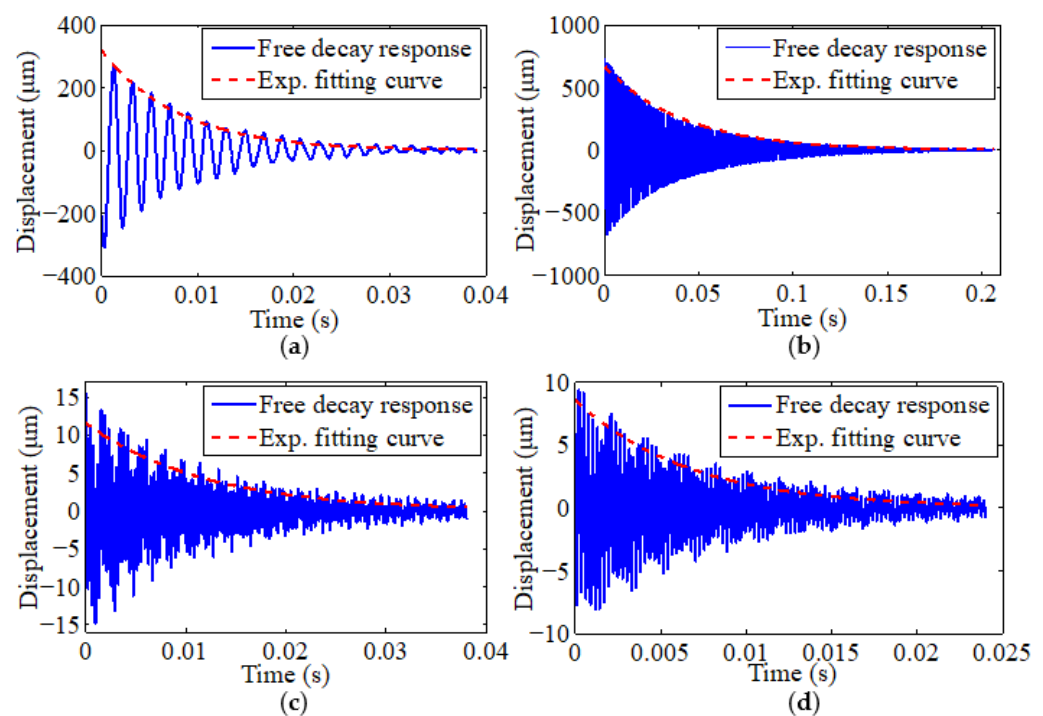


**Figure 5.** Calculated and tested amplitude–frequency response of torque motor with MF. (a) 0~2000 Hz; (b) 2000~4500 Hz.

**Table 4.** Identified resonance frequencies and modal damping ratios of armature assembly with and without MF.

Mode	Resonance Frequencies (Hz)		Modal Damping Ratios (%)	
	without MF	with MF	without MF	with MF
1st	523	512	3.76	11.38
2nd	1113	1101	0.34	0.91
3rd	2646	2623	0.50	0.94
4th	3752	3646	0.64	1.62

The tested resonance free decay responses of the torque motor with and without MF are shown in Figures 6 and 7. The modal damping ratios of the armature assembly can be identified using the identification algorithm described by Equation (1) to (6). The identified modal damping ratios are shown in Table 4.

**Figure 6.** Identified exponential decay curves vs. tested resonance free decay responses of torque motor without MF. (a) First mode; (b) second mode; (c) third mode; (d) fourth mode.

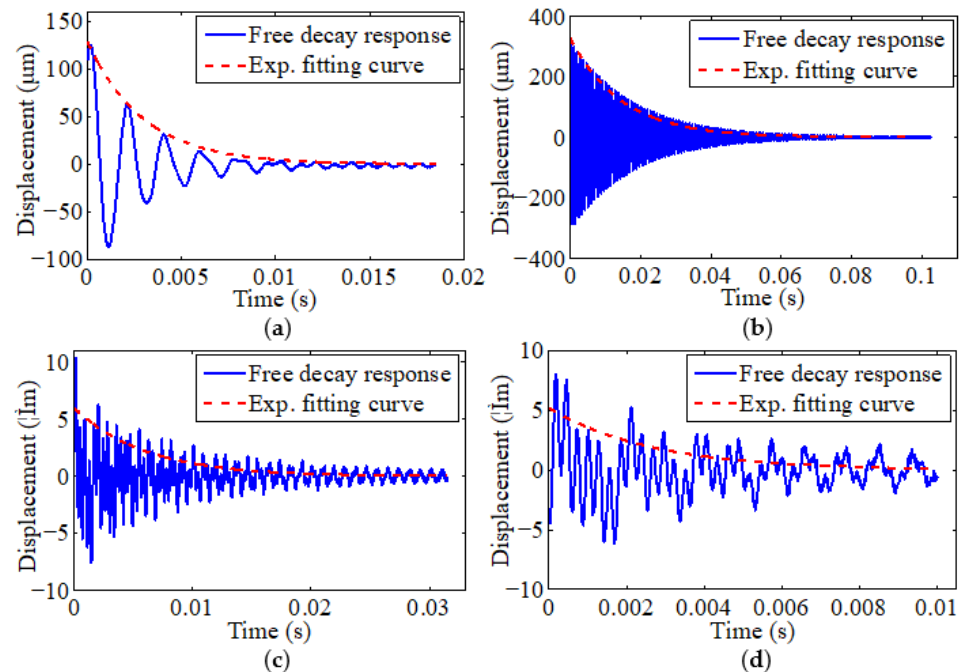
Figures 6 and 7 show that the identified exponential decay curves agree well with the peaks of the tested resonance free decay responses. It can be seen that the amplitudes of the free decay responses with MF decrease more rapidly. By comparing the identified modal damping ratios in Table 4, it is obvious that larger damping ratios are introduced to the armature assembly after MF is applied.

When MF is not added in the servo valve, the damping source of the armature assembly is mainly mechanical damping, while the damping source is the combination of mechanical and fluid damping after MF is added. From Table 4, we can see that the modal damping ratios are increased by double or more due to MF. The equivalent modal damping ratios due to squeeze flow of MF are achieved as 0.0662, 0.0065, 0.0051, and 0.0102, respectively. Thus, compared to the condition without MF, the damping ratios with MF are increased by 202.66%, 15.16%, 11.7%, and 26.06%, respectively.

Because the particles in MF are always magnetized to saturation in the working process of the servo valve, the viscosity of MF will always stay constant. However, the modal damping ratios vary with the resonance frequency. It can be seen that the added damping



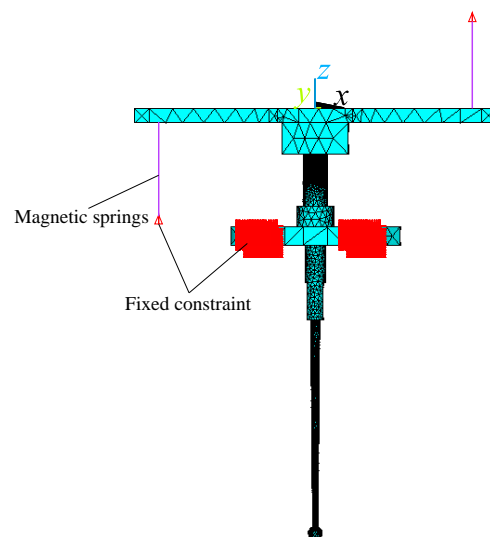
caused by MF is mainly distributed in the first vibration mode, while the added modal damping ratios are almost in a tenth level for the higher frequency range. Thus, when the MF works as a linear viscosity damper, the added modal damping ratios can be changed proportionally by selecting MF with different magneto-viscosity properties.



**Figure 7.** Identified exponential decay curves vs. tested resonance free decay responses of torque motor with MF. (a) First mode; (b) second mode; (c) third mode; (d) fourth mode.

### 5.2. Effect of MF on Resonance Amplitude

To verify the validity of the proposed modal damping ratio identification algorithm, numerical simulations are conducted using Ansys software. An equivalent finite element model of the armature assembly is established, as shown in Figure 8. The spring element COMBIN40 is used to simulate the function of magnetic spring induced by the electromagnetic torque of the torque motor [34]. The physical property for each component of the armature assembly is shown in Table 5.

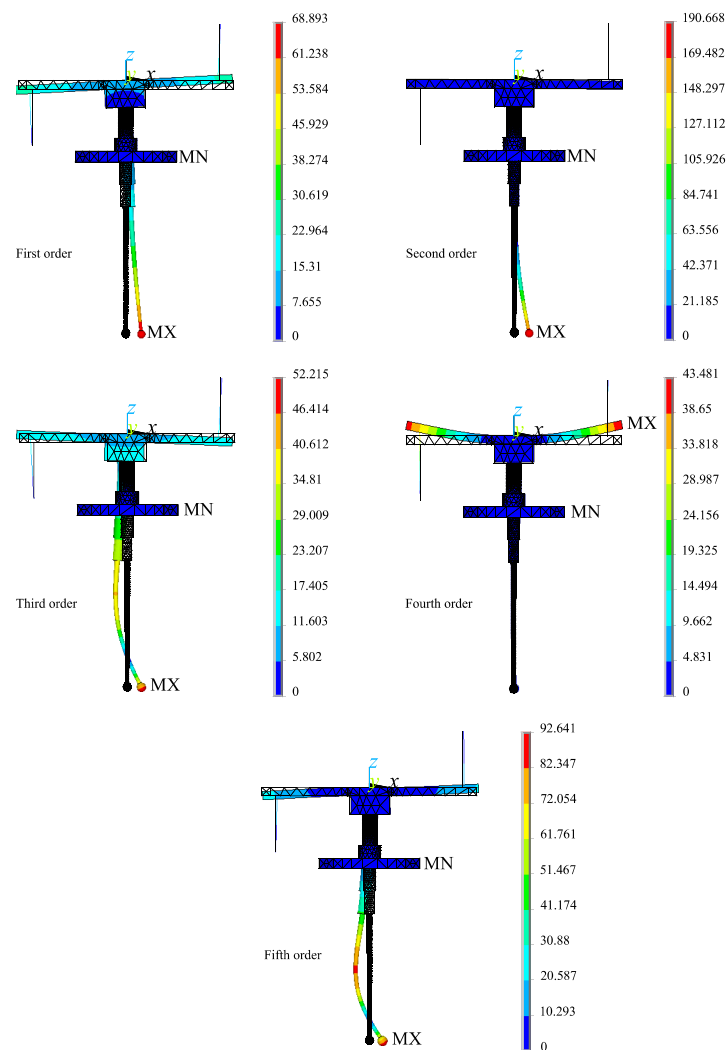


**Figure 8.** The finite element model of armature assembly.

**Table 5.** Physical property parameters of the armature assembly.

Component	Mass Density (kg/m <sup>3</sup> )	Young's Modulus (GPa)	Poisson's Ratio
Armature	8200	157	0.3
Spring pipe	8230	125	0.35
Flapper and Feedback rod	8000	190	0.3

Firstly, modal analysis is carried out to acquire the basic modal parameters (nature frequencies, vibration modes, etc.) of the armature assembly in the working plane ( $xoz$  plane). The simulated vibration modes of armature assembly with and without MF are almost the same in the frequency range from 0 to 4500 Hz. Figure 9 shows the vibration modes in the working plane ( $xoz$  plane) when MF is applied. It can be seen that the mode shapes in the working plane are mainly composed of the swing and bending of the armature assembly, and the maximum vibration displacement occurs at the end of the feedback rod or the armature. The vibration of the armature assembly becomes more distorted with the increase in modal order. The first order vibration mode is the overall swing of the armature assembly. For the second and fourth order modes, the lower order bending of the feedback rod or armature are dominant, while the third and fifth order modes are characterized as having higher order bending of the feedback rod and armature. The vibration modes also explain why only four resonance peaks are detected in the amplitude–frequency response curves.

**Figure 9.** Vibration modes of the armature assembly with MF in the working plane.

Based on modal analysis results and the identified modal damping ratios, the amplitude–frequency response of the armature assembly with and without MF can be calculated through harmonic response analysis using a modal superposition method.

The resonance amplitudes without and with MF are shown in Figures 4 and 5, respectively. It can be seen that a good agreement is achieved between the calculated and tested amplitude–frequency responses. In both responses, four resonance peaks appear in the frequency range of 0~4500 Hz, and the maximum resonance amplitude for both appears around 1100 Hz. The vibration energy dissipates gradually with the increasing frequency in the range of 2000~4500 Hz. It proves that the dynamic response of the armature assembly can be predicted accurately using the identified modal damping ratios.

As seen in Figures 4 and 5, the four resonance amplitudes are 301.8  $\mu\text{m}$ , 916.5  $\mu\text{m}$ , 13.9  $\mu\text{m}$ , and 9.3  $\mu\text{m}$ , when MF is not added. After MF is added in the servo valve, the four resonance amplitudes are 130  $\mu\text{m}$ , 318.7  $\mu\text{m}$ , 6.4  $\mu\text{m}$ , and 5.7  $\mu\text{m}$ , respectively. It can be seen that the resonance amplitudes are reduced by 56.9%, 65.2%, 53.9%, and 38.7%, respectively. Thus, it can be recognized that large damping forces have been introduced, and the stability of the torque motor can be increased by the application of MF.

## 6. Conclusions

The influence of applied MF on the modal damping ratios of the armature assembly in a hydraulic servo valve has been studied. Based on a resonance free decay response and Fourier series fitting method, an algorithm for identifying modal damping ratios is proposed. The proposed algorithm shows a high identification accuracy from 96.05% up to 98.74%, especially for the free decay response at the resonance frequency. By applying magnetic fluid ( $\text{Fe}_3\text{O}_4$ ) in the armature assembly, the damping ratios and resonance amplitudes are investigated. The equivalent modal damping ratios due to squeeze flow of MF are obtained through the proposed algorithm. The effect of MF is significantly found by improving the damping ratios of the armature by double or more. The added damping caused by MF is mainly distributed in the lower vibration mode. Based on the identified modal damping ratios, the amplitude–frequency responses can be estimated accurately, and the suppression mechanism of MF on resonance amplitudes of armature assembly can be explained.

The specific properties of MF can vary significantly with the type and concentration of the compositions. The validated method developed in this paper can provide a foundation for research on the further optimization of MF composition to achieve the best damping effect.

**Author Contributions:** Conceptualization, methodology, J.P. and S.L.; software, investigation, writing—original draft preparation, J.P. and Y.Z.; validation, writing—review and editing, S.L., W.B. and Y.T. All authors have read and agreed to the published version of the manuscript.

**Funding:** This research was funded by the National Key R&D Program of China, grant number 2020YFB2009701 and Open Foundation of the State Key Laboratory of Fluid Power and Mechatronic Systems, grant number GZKF-202025.

**Data Availability Statement:** The data presented in this study are available on request from the corresponding author.

**Conflicts of Interest:** The authors declare no conflict of interest.

## References

1. Abdallah, H.K.; Peng, J.; Li, S. Analysis of pressure oscillation and structural parameters on the performance of deflector jet servo valve. *Alex. Eng. J.* **2023**, *63*, 675–692. [[CrossRef](#)]
2. Tamburrano, P.; Plummer, A.R.; Palma, P.D.; Distaso, E.; Amirante, R. A novel servovalve pilot stage actuated by a piezo-electric ring bender: A numerical and experimental analysis. *Energies* **2020**, *13*, 671. [[CrossRef](#)]
3. Yang, Q.; Aung, N.Z.; Li, S. Confirmation on the effectiveness of rectangle-shaped flapper in reducing cavitation in flapper-nozzle pilot valve. *Energy Convers. Manag.* **2015**, *98*, 184–198. [[CrossRef](#)]

4. Lv, X.; Peng, J.; Li, S. Mathematical modeling of an armature assembly in pilot stage of a hydraulic servo valve based on distributed parameters. *Chin. J. Aeronaut.* **2021**, *34*, 50–60. [[CrossRef](#)]
5. Misra, A.; Behdinan, K.; Cleghorn, W.L. Self-excited vibration of a control valve due to fluid-structure interaction. *J. Fluids Struct.* **2002**, *16*, 649–665. [[CrossRef](#)]
6. Wang, Y.; Yin, Y. Performance reliability of jet pipe servo valve under random vibration environment. *Mechatronics* **2019**, *64*, 102286. [[CrossRef](#)]
7. Saha, B.K.; Peng, J.; Li, S. Numerical and experimental investigations of cavitation phenomena inside the pilot stage of the deflector jet servo-valve. *IEEE Access* **2020**, *8*, 64238–64249. [[CrossRef](#)]
8. Chen, M.; Xiang, D.; Li, S.; Zou, C. Suppression of squeal noise excited by the pressure pulsation from the flapper-nozzle valve inside a hydraulic energy system. *Energies* **2018**, *11*, 955. [[CrossRef](#)]
9. Wang, Y.; Chao, X.; Liu, G.; Hong, R.; Chen, Y.; Chen, X.; Li, H.; Xu, B.; Wei, D. Synthesis of Fe<sub>3</sub>O<sub>4</sub> magnetic fluid used for magnetic resonance imaging and hyperthermia. *J. Magn. Magn. Mater.* **2011**, *323*, 2953–2959. [[CrossRef](#)]
10. Li, Q.; Xuan, Y. Experimental investigation on heat transfer characteristics of magnetic fluid flow around a fine wire under the influence of an external magnetic field. *Exp. Therm. Fluid Sci.* **2009**, *33*, 591–596. [[CrossRef](#)]
11. Zhang, X.; Liu, L.; Qi, Y.; Liu, Z.; Shi, J.; Wen, W. Frequency-controlled interaction between magnetic microspheres. *Appl. Phys. Lett.* **2006**, *88*, 134107. [[CrossRef](#)]
12. Yang, W.; Li, D.; Feng, Z. Hydrodynamics and energy dissipation in a ferrofluid damper. *J. Vib. Control* **2013**, *19*, 183–190. [[CrossRef](#)]
13. Yao, J.; Chang, J.; Li, D.; Yang, X. The dynamics analysis of a ferrofluid shock absorber. *J. Magn. Magn. Mater.* **2016**, *402*, 28–33. [[CrossRef](#)]
14. Wang, Z.; Bossis, G.; Volkova, O.; Bashtovoi, V.; Krakov, M. Active control of rod vibrations using magnetic fluids. *J. Intell. Mater. Syst. Struct.* **2003**, *14*, 93–97. [[CrossRef](#)]
15. Saha, P.; Mukherjee, S.; Mandal, K. Rheological response of magnetic fluid containing Fe<sub>3</sub>O<sub>4</sub> nano structures. *J. Magn. Magn. Mater.* **2019**, *484*, 324–328. [[CrossRef](#)]
16. Ruan, X.; Pei, L.; Xuan, S.; Yan, Q.; Gong, X. The rheological responds of the superparamagnetic fluid based on Fe<sub>3</sub>O<sub>4</sub> hollow nanospheres. *J. Magn. Magn. Mater.* **2017**, *429*, 1–10. [[CrossRef](#)]
17. Pei, P.; Peng, Y. The squeeze strengthening effect on the rheological and microstructured behaviors of magnetorheological fluids: A molecular dynamics study. *Soft Matter* **2021**, *17*, 184–200. [[CrossRef](#)]
18. Becnel, A.C.; Sherman, S.G.; Hu, W.; Wereley, N.M. Squeeze strengthening of magnetorheological fluids using mixed mode operation. *J. Appl. Phys.* **2015**, *117*, 17C708. [[CrossRef](#)]
19. Liu, X.; Chen, Q.; Liu, H.; Wang, Z.; Zhao, H. Squeeze-strengthening effect of silicone oil-based magnetorheological fluid. *J. Wuhan Univ. Technol.-Mat. Sci. Ed.* **2016**, *31*, 523–527. [[CrossRef](#)]
20. Kezzar, M.; Tabet, I.; Nafir, N. Semi-analytical and numerical solutions for nonlinear problem of unsteady squeezing ferro-fluid flow between stretchable/shrinkable walls under external magnetic field and thermal radiation using differential transformation method. *J. Nanofluids* **2019**, *8*, 297–307. [[CrossRef](#)]
21. Sobamowo, M.G.; Akinshilo, A.T. On the analysis of squeezing flow of nanofluid between two parallel plates under the influence of magnetic field. *Alex. Eng. J.* **2018**, *57*, 1413–1423. [[CrossRef](#)]
22. Shafahi, M.; Ashrafi, N. Numerical investigation of a non-Newtonian fluid squeezed between two parallel disks. *Korea-Aust. Rheol. J.* **2020**, *32*, 89–97. [[CrossRef](#)]
23. Wang, N.; Liu, X.; Zhang, X. Squeeze-strengthening effect of silicone oil-based magnetorheological fluid with nanometer Fe<sub>3</sub>O<sub>4</sub> addition in high-torque magnetorheological brakes. *J. Nanosci. Nanotechnol.* **2019**, *19*, 2633–2639. [[CrossRef](#)]
24. Liu, Z.; Li, F.; Li, X.; Xu, J. Characteristic analysis and squeezing force mathematical model for magnetorheological fluid in squeeze mode. *J. Magn. Magn. Mater.* **2021**, *529*, 167736. [[CrossRef](#)]
25. Zhang, W.; Peng, J.; Li, S. Damping force modeling and suppression of self-excited vibration due to magnetic fluids applied in the torque motor of a hydraulic servovalve. *Energies* **2017**, *10*, 749. [[CrossRef](#)]
26. Li, S.; Bao, W. Influence of magnetic fluids on the dynamic characteristics of a hydraulic servo-valve torque motor. *Mech. Syst. Signal Process.* **2008**, *22*, 1008–1015. [[CrossRef](#)]
27. Peng, J.; Li, S.; Han, H. Damping properties for vibration suppression in electrohydraulic servo-valve torque motor using magnetic fluid. *Appl. Phys. Lett.* **2014**, *104*, 171905. [[CrossRef](#)]
28. Ishihara, T.; Wang, L. A study of modal damping for offshore wind turbines considering soil properties and foundation types. *Wind Energy* **2019**, *22*, 1760–1778. [[CrossRef](#)]
29. Grosso, P.; De Felice, A.; Sorrentino, S. A method for the experimental identification of equivalent viscoelastic models from vibration of thin plates. *Mech. Syst. Signal Proc.* **2021**, *153*, 107527. [[CrossRef](#)]
30. Zhang, L.; Hu, X.; Xie, Z. Identification method and application of aerodynamic damping characteristics of super high-rise buildings under narrow-band excitation. *J. Wind Eng. Ind. Aerodyn.* **2019**, *189*, 173–185. [[CrossRef](#)]
31. Tran, T.T.; Ozer, E. Synergistic bridge modal analysis using frequency domain decomposition, observer Kalman filter identification, stochastic subspace identification, system realization using information matrix, and autoregressive exogenous model. *Mech. Syst. Signal Process.* **2021**, *160*, 107818. [[CrossRef](#)]

32. Yao, X.J.; Yi, T.H.; Zhao, S.W. Blind modal identification for decentralized sensor network by modified sparse component analysis in frequency-domain subspace. *Eng. Struct.* **2022**, *269*, 114794. [[CrossRef](#)]
33. Sun, M.; Li, Q. Evaluation of modal properties of high-rise buildings under severe typhoon conditions using correlation function-based modal identification methods. *J. Wind Eng. Ind. Aerod.* **2022**, *229*, 105140. [[CrossRef](#)]
34. Merrit, H.E. *Hydraulic Control Systems*; John Wiley & Sons: New York, NY, USA, 1967.

**Disclaimer/Publisher's Note:** The statements, opinions and data contained in all publications are solely those of the individual author(s) and contributor(s) and not of MDPI and/or the editor(s). MDPI and/or the editor(s) disclaim responsibility for any injury to people or property resulting from any ideas, methods, instructions or products referred to in the content.